

CHAPTER II

LITERATURE REVIEW

The details of the Outokumpu flash smelting furnace, the concentrate burner, the oxygen pressure in the furnace, and chemical reaction occurring in the reaction shaft have been reviewed in this section. Previous literature on accretions have also been investigated.

2.1 OUTOKUMPU FLASH SMELTING FURNACE

Figure 2.1 shows a schematic drawing of the original Outokumpu flash furnace circuit. The furnace contains the following five major components:

- (i) concentrate burner which mixes dry concentrate with flux and O_2 -enriched blast, and directs the mixture downwards into the furnace;
- (ii) a reaction shaft where the reaction between O_2 and concentrate (Ni-(Cu)-Fe-S) takes place;
- (iii) a settler where the molten droplets form separate matte and slag layers;
- (iv) an off-take where SO_2 containing gases are removed from the

furnace;

(v) tapholes for removing matte and slag.

Most of the furnaces are contained in a steel casing about 1 cm. thick, with the exception of the reaction shaft roof and settler roof which are made of Cr_2O_3 -MgO refractory bricks packed around a refractory cover or water-cooled steel beams (Shima and Itoh, 1980). The interior lining of the furnace consists mainly of MgO and Cr_2O_3 -MgO refractory bricks. Normally, the reaction shaft and off take are water cooled to prevent heat loss and loss of strength in the furnace structure. The endwalls and side walls of the settler are cooled by water jackets or fins. Large portions of the settler are backed by water cooling to prevent refractory wear and overheating (Davenport *et al.*, 1984).

The integrated furnace at Kalgoorlie was built to resolve some of the difficulties in operation, as well as to improve the structure design and control the build up of hearth accretion (Elliot *et al.*, 1989). The hearth of the integrated flash furnace is extended along the same plane to include the slag reduction or appendage section. This replaces the separate slag reduction furnace in the original flash furnace. Figure 2.2 shows a comparison between the original flash furnace and integrated furnace layouts.

2.2. THE CONCENTRATE BURNER

The concentrate burners are located at the top of the reaction shaft. The function of the concentrate burner is to mix the furnace charge, flux and dry concentrates, with combustion air in the burner cone (Kemori *et al.*, 1985). Figure 2.3 (Kemori *et al.*, 1989) shows a conventional type of concentrate burner and its essential components. In recent years, a number of concentrate burners have been developed to overcome operational difficulties and give increased operational capacity. Oxygen gas was used to reduce the air speed (due to the reduction of the air volume) and supplementary fuel. This causes a decrease in the mixing energy, so that the mixing energy per unit weight of the furnace charge becomes small (Kemori *et al.*, 1985).

Figure 2.4 (Kemori *et al.*, 1989) shows a drawing of a new type of concentrate burner. The air speed regulator is a device that controls the air velocity to maintain mixing at high oxygen enrichment. The burner used in the Kalgoorlie Nickel Smelter is shown in Figure 2.5 (Elliot *et al.*, 1989). This concentrate burner has been modified to overcome problems relating to the effective gas-solids mixing and melting capacity. It relies on air dispersion of the charge using high pressure air on a distributor cone (Elliot *et al.*, 1989).

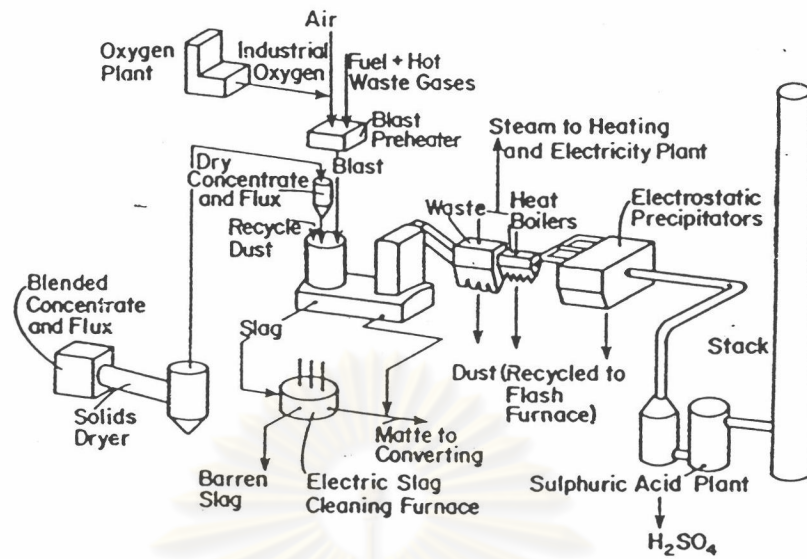


Figure 2.1 Schematic drawing of the original Outokumpu flash smelting circuit (Davenport *et al*, Flash Smelting, 1984).

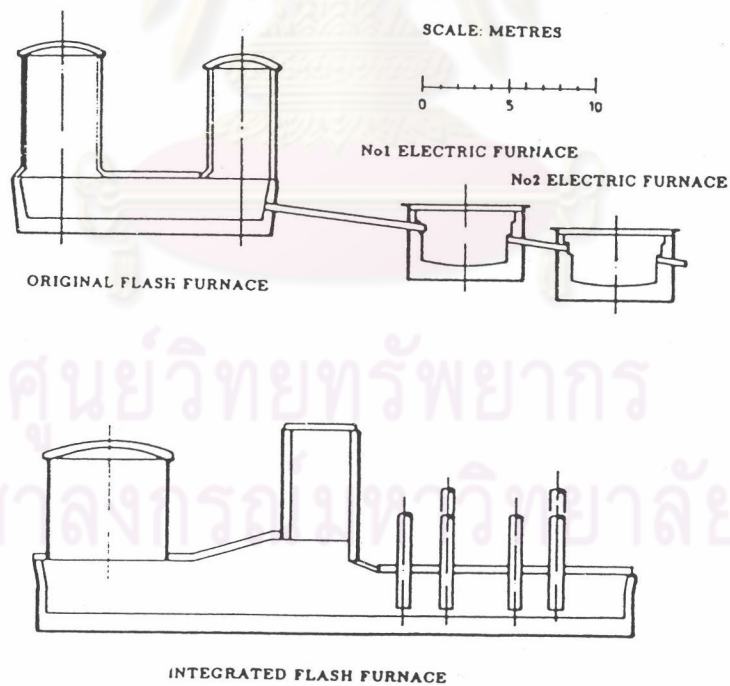


Figure 2.2 Comparison between the original flash furnace and integrated furnace layouts. (Elliot *et al.*, 1989)

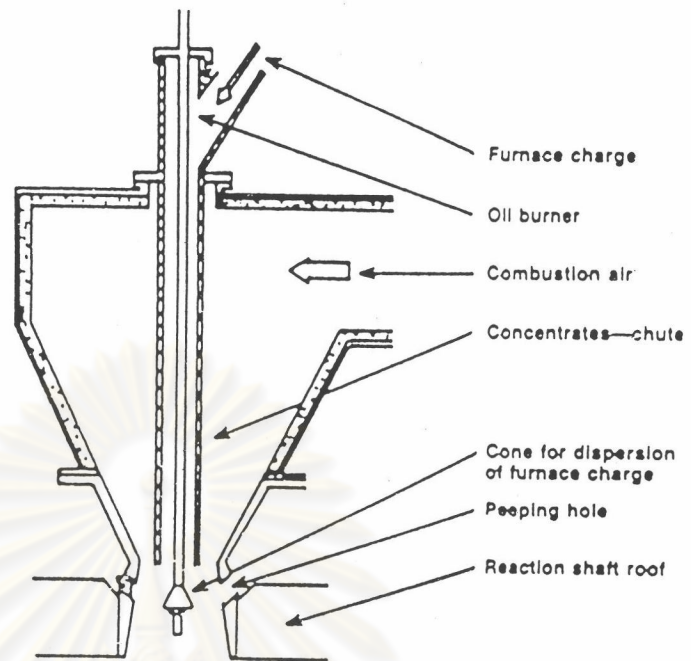


Figure 2.3 Conventional type concentrate-burner.

(Kemori *et al*, 1985)

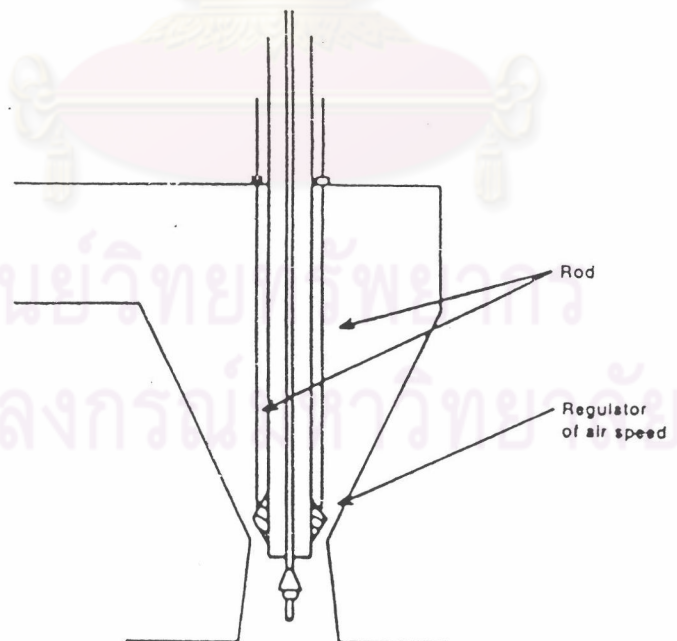


Figure 2.4 New type of concentrates-burner with the regulator.

2.3 CHEMICAL REACTIONS IN FLASH SMELTING

The feed for the Kalgoorlie flash furnace are nickel sulphide concentrates from Kambalda, Agnew and Windarra, silica flux, lateritic material (nickel silicate) and coal dust. The major phases present are pentlandite $(\text{FeNi})_9\text{S}_8$, violarite $(\text{NiFe}_2\text{S}_4)$, Pyrrhotite $(\text{Fe}_{1-x}\text{S})$, Pyrite (FeS_2) and some minor phases such as iron oxides and magnesium silicates (Pleysier, 1985).

The concentrates are fed into the furnace through the burners at the top of reaction shaft. Most of reactions occur in the reaction shaft at a temperature between $1,350\text{ }^\circ\text{C}$ to $1,400\text{ }^\circ\text{C}$. The feed materials are oxidized producing a nickel-iron oxide and iron sulphides which drop to the settler below the reaction shaft. The iron sulphides are oxidized continuously to iron oxides. The iron sulphides also react with magnetite (Fe_3O_4) to give iron oxide (FeO) and sulfur dioxide (Kemori *et al.*, 1986). The oxidation reactions are listed in Table 2.1. The iron oxides react with the silica flux in the settler to form a slag which flows towards the slag cleaning section.

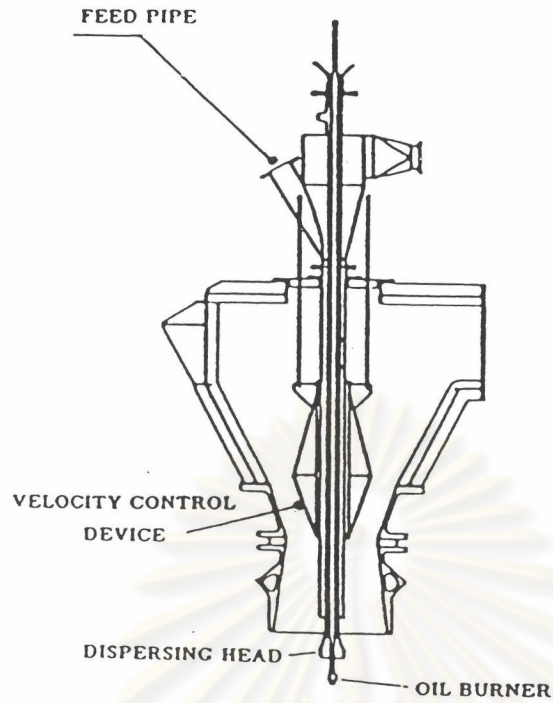


Figure 2.5 Modified Venturi -Type Burner

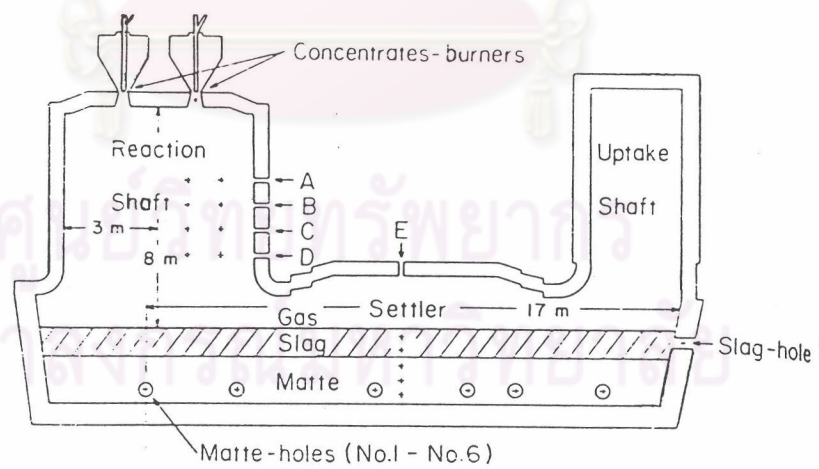
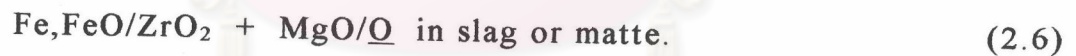


Figure 2.6 Flash smelting furnace showing location of emf measurements (Kemori *et al.*, 1986)

Table 2.1 Chemical reaction in the reaction shaft

| Reaction | [EQ] |
|--|------|
| $\text{FeS}_2 + (5/2)\text{O}_2 = 2\text{SO}_2 + \text{FeO}$ | 2.1 |
| $\text{NiS} + (3/2)\text{O}_2 = \text{NiO} + \text{SO}_2$ | 2.2 |
| $\text{FeS} + (3/2)\text{O}_2 = \text{FeO} + \text{SO}_2$ | 2.3 |
| $3\text{Fe}_3\text{O}_4 + \text{FeS} = 10\text{FeO} + \text{SO}_2$ | 2.4 |
| $2\text{FeO} + \text{SiO}_2 = 2\text{FeO} \cdot \text{SiO}_2$ | 2.5 |

Kemori *et al.* (1986) have studied the reaction mechanism in the Toyo copper flash smelting furnace by using a galvanic cell. The galvanic cell used in this study is described schematically as;

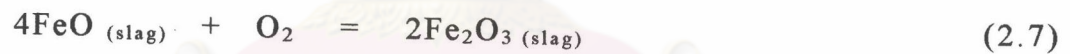


This study considered the reactions among concentrate particles, without particle recycling in the reaction shaft at the positions shown in Figure 2.6. Most of the oxidation of the concentrates occurred in the upper zone of the reaction shaft and are completed at about 3 meters below the shaft roof. Some oxidized concentrate particles melt owing to the heat produced by the reaction but other concentrate particles probably are oxidized, but not melted. When molten

particles collide with the less oxidized solid particles, there is a transfer of energy resulting in the formation of a single molten particle. There will also be an oxidation reaction as the components of the original particles equilibrate. This reaction will continue until the equilibrium is attained. Figure 2.7 shows silica flux (SiO_2) reacting with the oxidized particles in the final stage.

2.4 OXYGEN PARTIAL PRESSURE IN FLASH SMELTING

Floyd *et al.* (1979) have studied the state of oxidation of high iron slag produced in non-ferrous smelting using disposable-tip emf cells. The oxygen potential in slag is controlled by the equilibrium:



Thus, the oxygen potential ($\mu(\text{O}_2)$) in slag should be explained by the relationship:

$$\mu(\text{O}_2) = RT \ln p(\text{O}_2) \quad (2.8)$$

$$= \Delta G^\circ_{(7)} + RT \ln [a^2(\text{Fe}_2\text{O}_3) / a^4(\text{FeO})] \quad (2.9)$$

Where $\Delta G^\circ_{(7)}$ is the standard free energy change for equation 2.7.

'a' is the activity of each species.

It can be seen in Figure 2.8 that the oxygen potential decreased along the length of the flash furnace. The decrease in oxygen potential may have been due either to reduction of slag by electrode carbon or the presence of slag along the sides of the furnace (Floyd *et al.*, 1979).

Kemori *et al.* (1985) investigated the oxygen potential in the copper flash furnace. The oxygen pressure decreased from 10^{-3} to 10^{-9} atmosphere at 1523 K along the vertical axis from the reaction shaft roof to settler bottom. Kemori *et al.* (1989) have also studied the oxygen partial pressure in the settler and electric furnace by using a galvanic cell. The vertical variation of oxygen pressure in slag, matte and reaction shaft in the flash furnace was studied at point A to E in Figure 2.6. The oxygen partial pressure gradually decreased from the gas/slag interface to the slag/matte interface and increase from the slag/matte interface to the settler bottom. The results of this study are shown in Figure 2.9. The influence of recycled dust on oxygen pressure (Kemori *et al.*, 1986) are shown in Figure 2.10. For furnace operation without recycled dust, the oxygen pressure at holes A in Figure 2.6 is lower than oxygen pressure at hole B through to D in Figure 2.6. On the other hand, the oxygen pressure at hole A is higher than Hole B through to D for furnace operation with recycled dust (Figure 2.10).

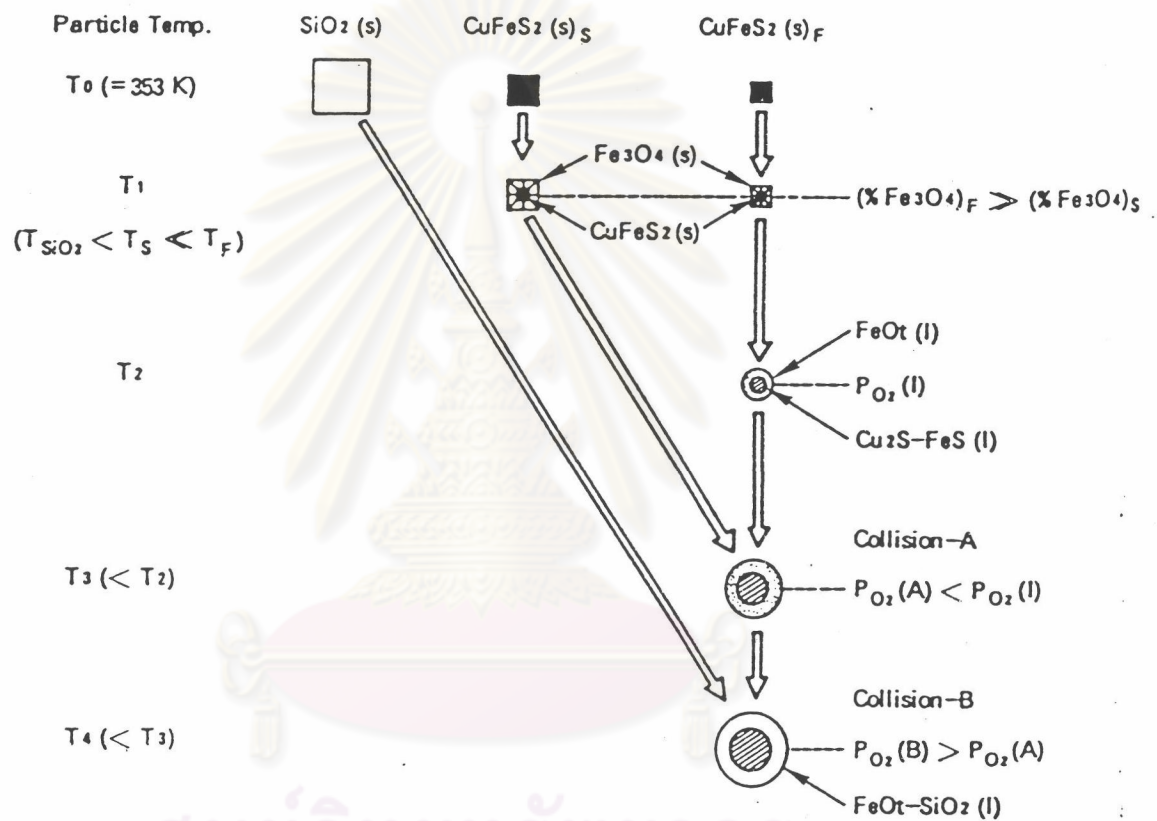


Figure 2.7 Reaction mechanism in the reaction shaft.

F = fast reacting and S = slow reacting

(Kemori *et al.*, 1989).

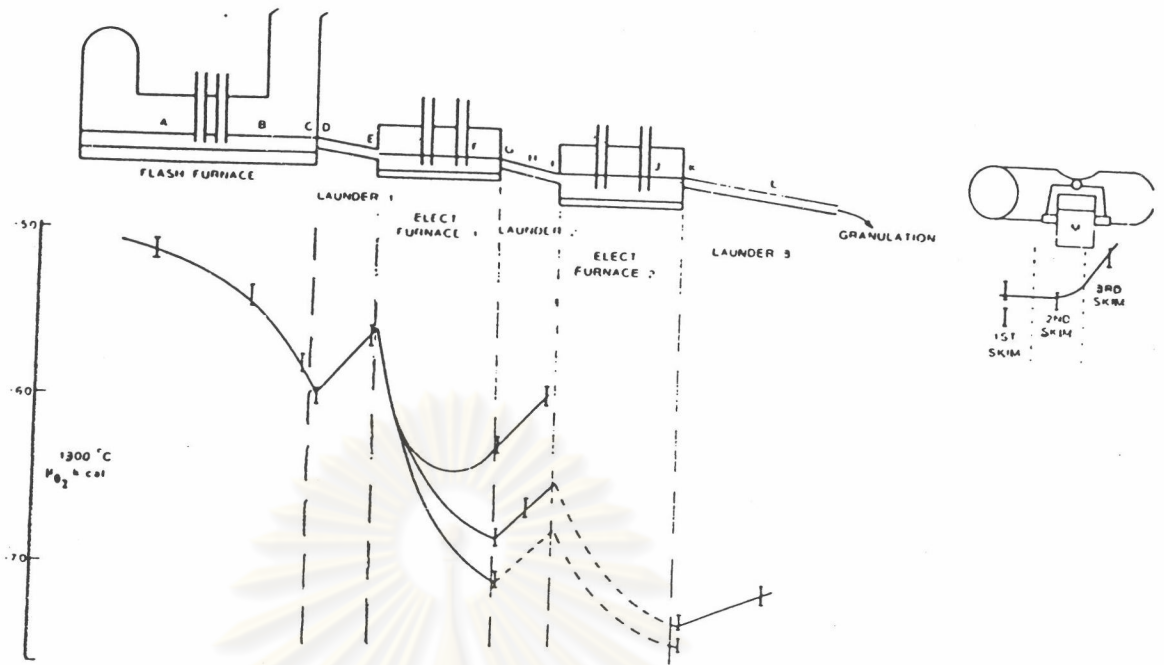


Figure 2.8 Schematic diagram of oxygen potential variation along the furnace (Floyd *et al.*, 1979).

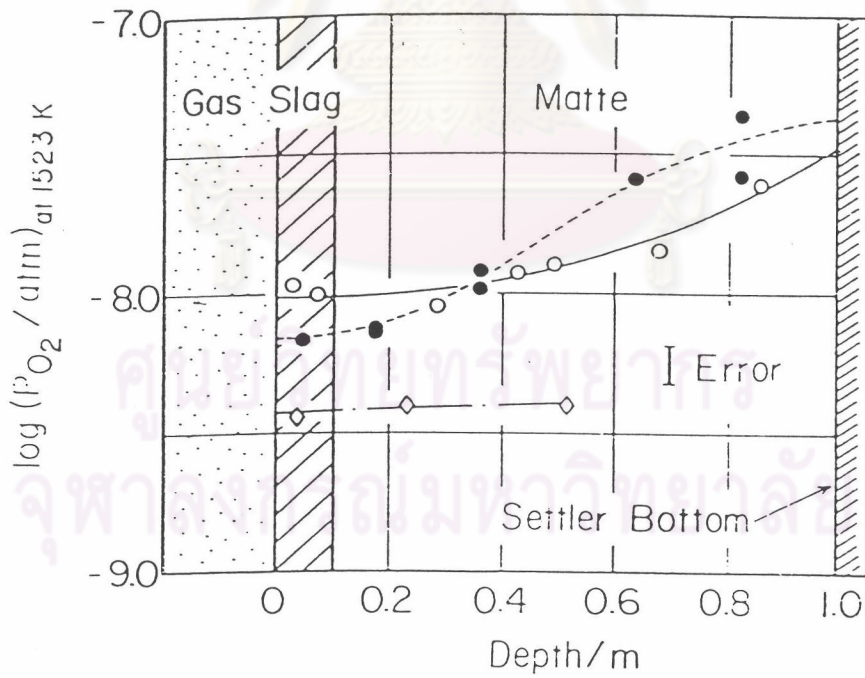


Figure 2.9 Variation of oxygen partial pressure at 1523 K with depth from the slag surface (Kemori *et al.*, 1986)

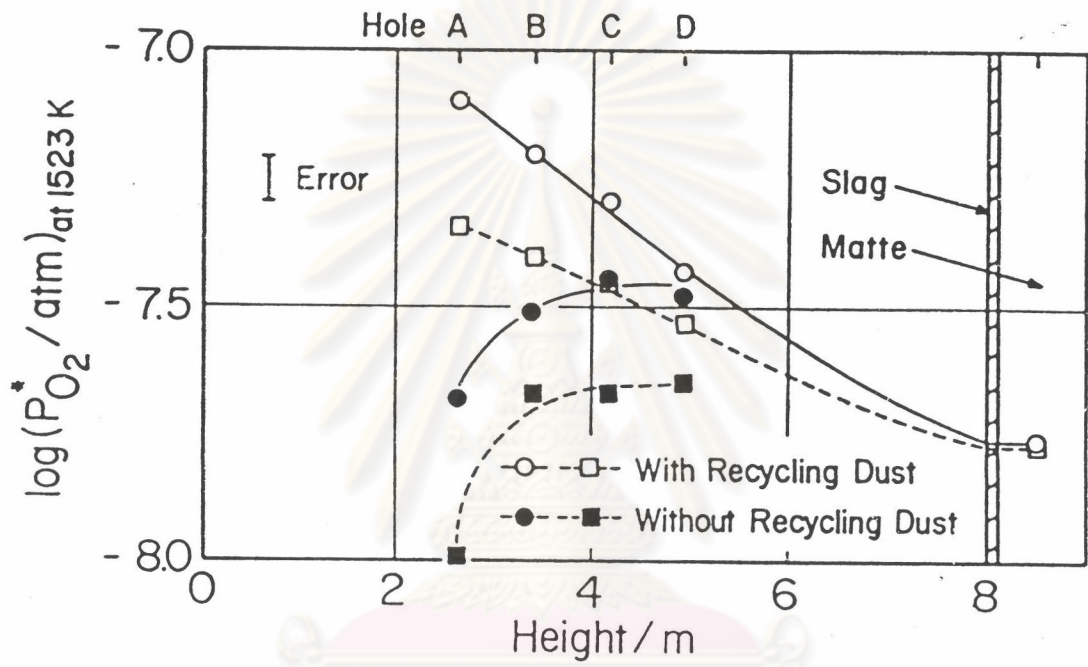


Figure 2.10 Influence of Recycled Dust on Oxygen Pressure

(Kemori, 1986)

2.5 CHEMISTRY OF ACCRETIONS AND PREVIOUS EXPERIMENTS.

Segnit (1976) has studied the chemical composition of nickel slag and accretion from the base and wall of the Kalgoorlie flash furnace. It was found that the dominant phase in the accretions from the base of the furnace is magnetite with some olivine also present. The partial reduction of magnetite to wustite had occurred in some cases. In the interstitial glass, pyroxene occurred as dendritic growths. The oxide and silicate phases contained little nickel. The accretions from the wall of the furnace consisted mainly of a porous aggregate of grains of a magnetite-like phase cemented by olivine ($2(\text{Mg,Fe})\text{O} \cdot \text{SiO}_2$) and little glass. All phases were rich in nickel. The olivine had a high nickel content, and contained little magnesium. As well as the interstitial silica material which was rich in calcium, iron, and nickel, a spinel nickel ferrite (NiFe_2O_4), and a copper nickel oxide, $(\text{Cu, Ni})\text{O}$, were found in this study.

George-Kennedy (1984) studied the physical and chemical factors affecting accretions in the uptake shaft and throat. Accretion samples from the throat of uptake shaft (see Figure 4.1) were collected by three methods as follows;

ASDST - dust collected by vacuum pump and filter:

ASACC - accretions collected on a water-cooled probe projected into the gas train.

ASLIQ - the liquid flowing down the throat was collected by a bar projected across from the sampling point to the opposite wall.

Accretions collected by ASLIQ were classified into 5 types as follows,

Type 1 - brittle and friable material.

Type 2 - physical properties looked like type 1 but had bands of molten strata.

Type 3 - hard material with a porous-looking structure. A fine crystalline structure was observed with some evidence of total fusion in parts.

Type 4 - samples similar to type 3 but the density was greater.

Type 5 - massive material, no porosity and very heavy.

The main phase in types 3 to 5 was a mixed spinel. In type 3, nickel-fayalite-forsterite was a common phase, with free silica appearing in some areas. The presence of silica and fayalite in the type 3 accretions tends to suggest that this sample was chilled somehow within the throat (George-Kenedy, 1984). Type 4 accretions show a eutectoid type structure between the silica and the nickel-fayalite-forsterite phase. The eutectoid structure probably shows the different

thermal history between type 3 and type 4 accretions. The eutectoid structure exhibited in type 4 could be the result of very slow cooling. The type 5 accretion exhibited a matrix of fayalite. There was no explanation of the effect of the fayalite matrix on the physical properties.

Pleysier (1985) prepared accretions using a simulated flash furnace, by passing nickel concentrate from the Kambalda Nickel Operation (KNO) through a simulated flash furnace at different feed rates and air temperature. The phases present in the accretion were identified by XRD as hematite and magnetite or nickel spinel. The addition of 20 % wt. silica flux in the feed did not produce metal silicate phases in the products and had no affect on the formation of accretions in the simulated furnace.

2.6 METAL OXIDE SYSTEMS RELEVANT TO ACCRETIONS.

2.6.1 Fe-Ni-O System

Figure 2.11 (Pelton *et al.*, 1971) shows the phase diagram for the Fe-Ni-O system at 1065 K to 1378 K. The system is characterised by a two alloy phase (α alloy and γ alloy) at 1065 K and lower oxygen partial pressure. Hematite (Fe_2O_3) regions are present at

1277 K and high oxygen partial pressure (Figure 2.11). Above the wustite-magnetite equilibrium shown in Figure 2.12, wustite has disappeared and has been replaced by spinel (Ono *et al.*, 1979). Smeltser *et al.* (1970) found nickel content to be slightly lower in wustite than in the spinel.

Naldrett (1972) found that nickel olivine (Ni_2SiO_4) forms a continuous series of solid solutions with Fe_2SiO_4 at 900 C. They also found that silica stabilizes iron oxide (FeO) and nickel oxide (NiO) in the reaction;



The Ni_2SiO_4 is stable up to 1545° C and Ni_2SiO_4 does not appear at high nickel content (Phillip *et al.*, 1963). Shaw and Willis (1975) found that there is no solubility of silica in the oxide phase of the Fe-Ni-O system.

2.6.2 Fe-Si-Mg-O System

The original studies of the FeO-SiO₂-MgO system were made by Bowen *et al.* (1932). They found that there is a solid solution extending from enstatite (MgSiO₃) part way towards Fe₂SiO₄ in the

system (Broadbent *et al.*, 1993). The effect of the addition of magnesium in the Fe-Si-O system is to increase the liquidus temperature. Any increment of magnesium oxide increases the melting point of the material. At 5 percent magnesium oxide, the liquidus temperature is increased by approximately 50° C (George-Kennedy, 1984). The effect of decreasing oxygen pressure on the Fe-Mg-Si-O ternary system is shown in Figure 2.13. The region of iron in the ferric state decreased with decreasing oxygen partial pressure and is replaced by olivine and magnesiowustite at a CO₂/H₂ ratio equal to 19.

2.7 SUMMARY

Flash smelting was developed in the 1940s by Outokumpu Oy in Finland. It is currently used for extracting the copper and nickel from sulphide concentrates to matte before refinement to metals. There are five major components in a flash smelter including the reaction shaft in which most concentrates react with oxygen to give matte and slag in the settler. In Kalgoorlie, Western Australia, the integrated flash furnace is used to produce nickel matte. The feed for the flash smelting furnace is introduced into the furnace with fuel and oxygen in the burners at the top of the reaction shaft. The function of the concentrate burner is to mix the furnace charge with combustion air. The burner design has been developed to improve the gas-solid mixing

and the melting capacity. The concentrate burner can be classified into three type as shown in Figures 2.3 to 2.5. In the reaction shaft, the sulphide concentrates are oxidized and transform to oxides which collect in the settler.

Accretions form in different areas of the flash furnace including the throat, the appendage, settler and reaction shaft. The dominant phases in the accretions are iron-silica oxides with high nickel and magnesium, and iron oxides with high nickel content.

The oxygen partial pressure in the flash furnace varies in the vertical and horizontal directions. The oxygen partial pressure decreased from 10^{-3} atmosphere at the top of the reaction shaft to 10^{-9} atmosphere at the slag surface in the settler. The oxygen pressure in the appendage is lower than in the settler. The literature review shows that there is no information regarding the structure of accretions formed in different regions of the furnace, and there is no information reported on the effect of system conditions (temperature, oxygen partial pressure) on the accretion microstructure and mechanism of accretion build up in furnace.

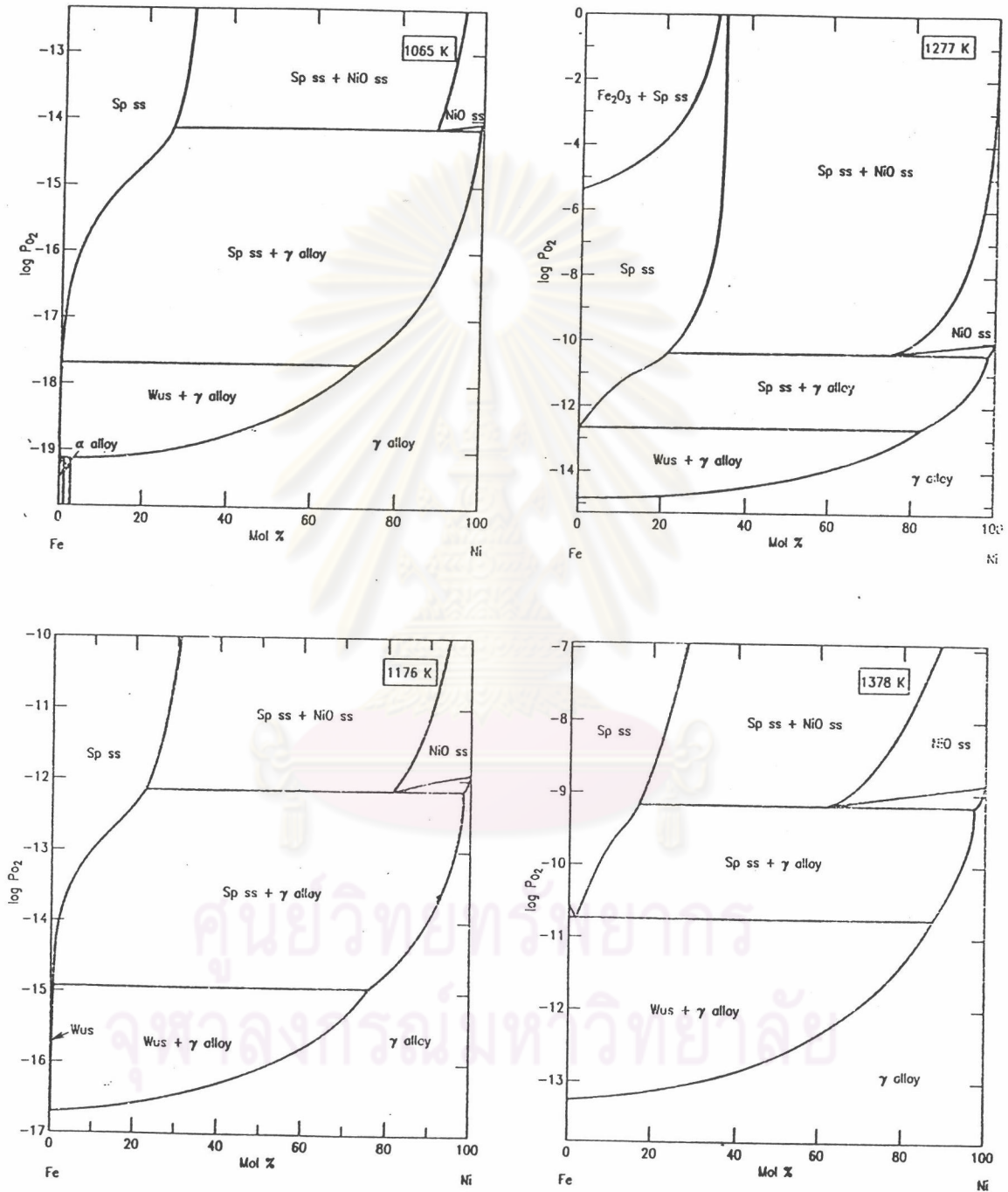


Figure 2.11 Ternary Diagram of System Fe-Ni-O (Pelton *et al.*, 1979)

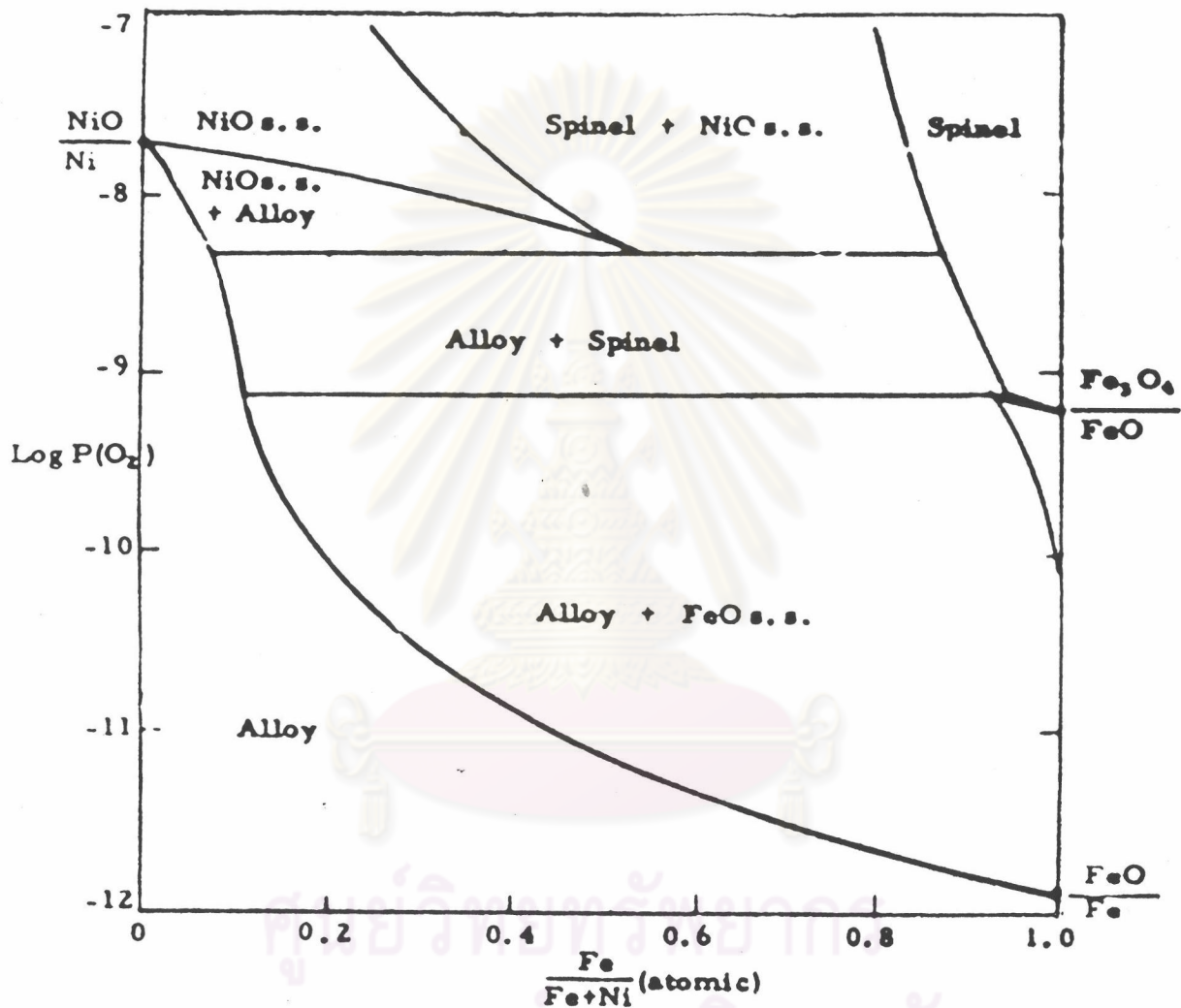


Figure 2.12 Ternary Diagram of System Fe-Ni-O at 1277° C

(Shaw and Willis, 1975)

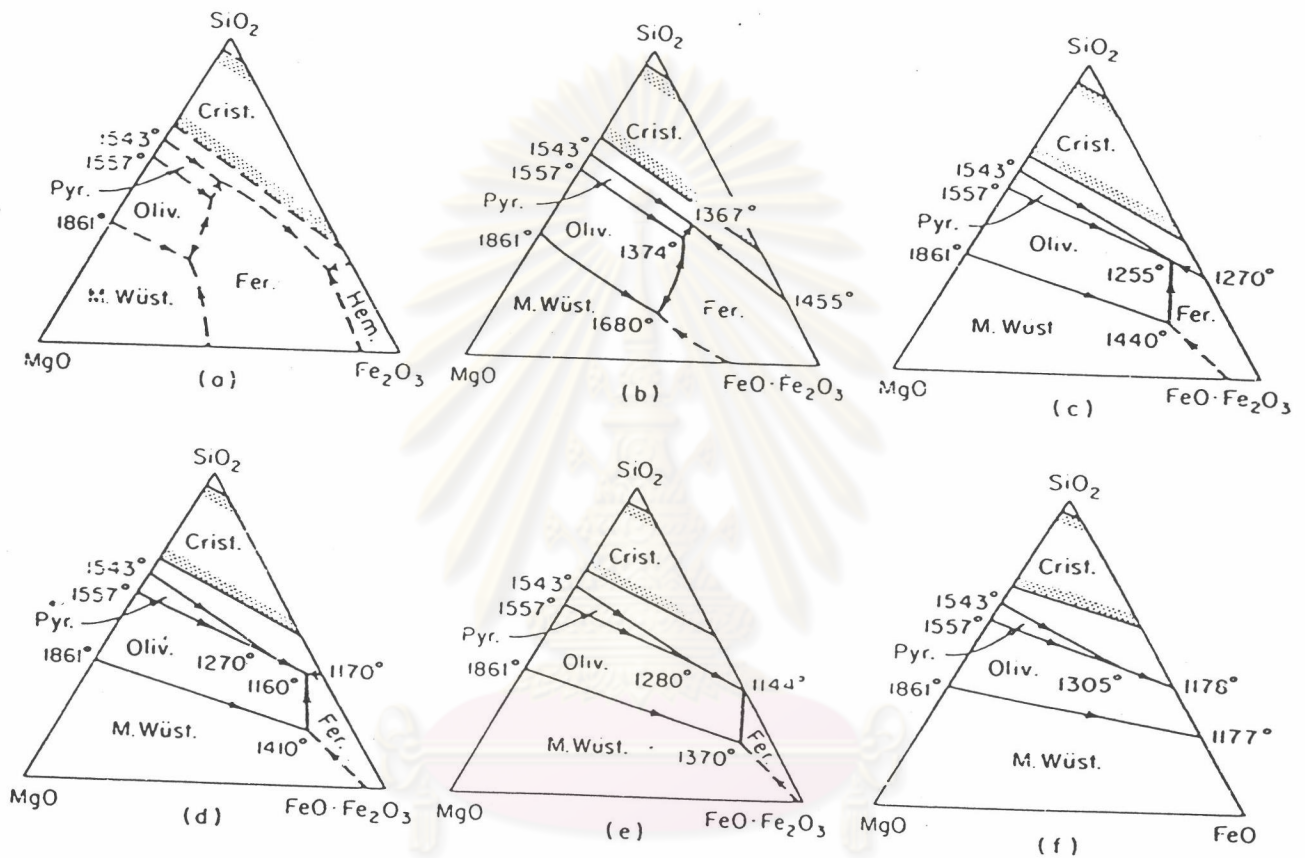


Figure 2.13 The system $\text{FeO-MgO-Fe}_2\text{O}_3\text{-SiO}_2$ with decreasing oxygen pressure (a) at sufficiently high O_2 pressure to keep essentially all of the iron in the ferric state. (b) in air, (c), (d), and (e) at constant CO_2/H_2 ratio of 40, 24 and 19, respectively. (f) extreme reducing conditions of melts in contact with metallic iron.

(Arnulf Muan and E.F. Osborn, 1956).